Coral Reefs
DOI 10.1007/s00338-011-0833-4

REPORT

Transcriptomic responses to darkness stress point to common coral bleaching mechanisms

M. K. DeSalvo · A. Estrada · S. Sunagawa · Mónica Medina

Received: 16 April 2011 / Accepted: 7 October 2011

Abstract Coral bleaching occurs in response to numerous abiotic stressors, the ecologically most relevant of which is hyperthermic stress due to increasing seawater temperatures. Bleaching events can span large geographic areas and are currently a salient threat to coral reefs worldwide. Much effort has been focused on understanding the molecular and cellular events underlying bleaching, and these studies have mainly utilized heat and light stress regimes. In an effort to determine whether different stressors share common bleaching mechanisms, we used complementary DNA (cDNA) microarrays for the corals *Acropora palmata* and *Montastraea faveolata* (containing >10,000 features) to measure differential gene expression during darkness stress. Our results reveal a striking transcriptomic response to darkness in *A. palmata* involving chaperone and antioxidant up-regulation, growth arrest, and metabolic modifications. As these responses were previously measured during thermal stress, our results suggest that different stressors may share common bleaching mechanisms. Furthermore, our results point to hypoxia and endoplasmic reticulum stress as critical cellular events involved in molecular bleaching mechanisms. On the other hand, we identified a meager transcriptomic response to darkness in *M. faveolata* where gene expression differences between host colonies and sampling locations were greater than differences between control and stressed fragments. This and previous coral microarray studies reveal the immense range of transcriptomic responses that are possible when studying two coral species that differ greatly in their ecophysiology, thus pointing to the importance of comparative approaches in forecasting how corals will respond to future environmental change.

Keywords Coral bleaching · Microarrays · Transcriptomics · Darkness stress · Symbiosis · Coral reefs

Communicated by Environment Editor Prof. Rob van Woesik.

Electronic supplementary material The online version of this article (doi:10.1007/s00338-011-0833-4) contains supplementary material, which is available to authorized users.

M. K. DeSalvo · A. Estrada · S. Sunagawa · M. Medina (✉)
School of Natural Sciences, University of California Merced, 5200 North Lake Road, Merced, CA 95343, USA
e-mail: mmedina@ucmerced.edu

Present Address:
M. K. DeSalvo
Department of Anesthesia, UCSF School of Medicine, Mission Bay Campus, 600 16th St., Box 2200, San Francisco, CA 94158, USA

Present Address:
S. Sunagawa
European Molecular Biology Laboratory, Meyerhofstraße 1, 69117 Heidelberg, Germany

Introduction

Coral bleaching describes the paling of a coral colony due to the loss of their endosymbiotic algae (*Symbiodinium* spp.) and/or degradation of algal photosynthetic pigments (Hoegh-Guldberg 1999). Stressors known to cause bleaching include anomalous water temperature and salinity, excessive solar irradiation, and exposure to heavy metals and herbicides (reviewed in e.g., Brown 1997; Douglas 2003; Weis 2008). Coral mortality does not necessarily occur following bleaching events; in fact, some coral species can increase their heterotrophic feeding rates in order to make up for the lost energy usually provided by their endosymbiotic algae (Grottoli et al. 2006). However, intense bleaching events can dramatically decrease live coral cover over large geographic

Published online: 20 October 2011

areas (Hoegh-Guldberg 1999). Since scleractinian corals build the three-dimensional framework of the reef ecosystem and their symbiotic relationship with *Symbiodinium* drives the immense productivity and biodiversity of coral reefs, bleaching-induced reef degradation represents a critical threat to the survival of coral reefs.

Due to the ecological importance of reef-building corals, understanding the physiologic, cellular, and molecular underpinnings of the bleaching phenomenon represents a paramount research objective for coral researchers. As described in Douglas (2003), the bleaching response can be broken into three events: triggers, mechanisms, and symptoms. The *triggers* are the abiotic stressors mentioned above, and the most likely *mechanism* involves reactive oxygen species (ROS) formation in the chloroplasts of *Symbiodinium* and the mitochondria of both host and endosymbiont (Lesser 1996; Nii and Muscatine 1997; Tchernov et al. 2004, 2011; Higuchi et al. 2011; Saragosti et al. 2011; Wang et al. 2011). The cytotoxic ROS lead to bleaching, which is marked by the following *symptoms*: exocytosis (Steen and Muscatine 1987), cell detachment (Gates et al. 1992), apoptosis or necrosis of host cells (Dunn et al. 2002, 2004, 2007) or *Symbiodinium* cells (Dunn et al. 2002, 2004; Strychar et al. 2004), and in situ degradation of the *Symbiodinium* cells via autophagy (Dunn et al. 2007; Downs et al. 2009). Missing in this series of events are the exact molecular *mechanisms* (i.e., cellular signaling cascades) linking ROS activity to the *symptoms* mentioned above.

Recent advances in coral genome biology have greatly expanded our knowledge of the molecular and cellular events surrounding coral stress and bleaching. cDNA microarray experiments focusing on thermal stress and bleaching in adult *Montastraea faveolata* (DeSalvo et al. 2008, 2010b) and *Acropora palmata* (DeSalvo et al. 2010a) have revealed coral host responses during stress and bleaching such as up-regulation of antioxidant proteins and chaperones, down-regulation of calcium-binding proteins and ribosomal proteins, and modifications to the actin cytoskeleton and extracellular matrix. The identification of these core processes conserved in the coral bleaching response required an evolutionary comparative approach. Another approach for the identification of core bleaching mechanisms is to perform bleaching experiments using other stressors such as darkness, salinity, and cold shock. By adopting this strategy, one can determine whether different triggers share common mechanistic components (Douglas 2003).

In this study, we measured differential gene expression using cDNA microarrays in fragments of *A. palmata* and *M. faveolata* kept in complete darkness for 9 and 10 days, respectively. As the first coral microarray study aimed at darkness-induced bleaching, we compare our results to those generated under thermal stress conditions with the goal of elucidating shared mechanisms underlying two different bleaching stressors.

Materials and methods

For further details on all methodologies, please see the Electronic Supplemental Material, ESM Text.

Field experiments

The field experiments were performed at the Smithsonian Tropical Research Institute's Bocas del Toro field station in Panamá during September and October 2006. Large fragments from four colonies of *M. faveolata* were sampled from two reefs 21.4 km apart (two from Isla Solarte—9°19′59.58″N and 82°13′6.70″W—which are referred to as colonies 1 and 2 and two from Cayos Zapatillas—9°15′8.07″N and 82°2′26.76″W—which are referred to as colonies 3 and 4). In addition, four colonies of *A. palmata* were sampled from two reefs 8.3 km apart (two colonies from the "Crawl Cay" reef—9°15′N and 82°07′W and two colonies from Cayos Zapatillas). In the case of *A. palmata*, information regarding the reef of origin was lost.

Tank experiments were performed concurrently with the experiments described in DeSalvo et al. (2008) and (2010a), and thus, the methods are nearly identical. Following a 4-day acclimation period, a fragment from each control and experimental aquaria for each species was sampled (t0-C and t0-D). After time zero sampling, the experimental tanks were covered with black plastic to eliminate all ambient light. After 9 and 10 days of darkness stress, a fragment of *A. palmata* and *M. faveolata*, respectively, was sampled from each control and experimental aquaria (9d-C and 9d-D for *A. palmata* and 10d-C and 10d-D for *M. faveolata*). All samples were taken at night between 18:00 and 20:00 h and frozen in liquid nitrogen. Immediately prior to freezing, a polyp-size tissue scraping ($\sim$12.6 mm^2) was preserved in 3.7% formaldehyde.

Symbiodinium cell density measurements and genotyping

The formaldehyde-fixed tissue scrapings were homogenized, and *Symbiodinium* cells were counted using a hemocytometer. For both species, an ANOVA model was set up to test for the effects of time, tank, and the interaction between time and tank. Post hoc testing via the Tukey HSD method on the interaction term determined which time–tank combinations were significantly different from each other.

Genomic DNA was isolated from frozen coral powder using the PowerPlant DNA Isolation kit (MoBio). *The*

Symbiodinium 18S ribosomal RNA gene was amplified from all samples using the primers ss5 and ss3Z (Rowan and Powers 1991), digested with TaqI restriction enzyme, and compared with *Symbiodinium* standards (Rowan and Knowlton 1995).

Microarray laboratory and data analysis techniques

Total RNA from all frozen coral fragments was isolated using QIAzol lysis reagent (Qiagen), and quantity and quality were assessed using previously published protocols (DeSalvo et al. 2010a). The *A. palmata* microarrays used in this study consisted of 13,546 PCR-amplified cDNAs that were spotted in duplicate; the *M. faveolata* microarrays consisted of 10,930 cDNAs that were also spotted in duplicate. These new, larger microarrays consist of spotted cDNAs chosen from older libraries described in Schwarz et al. (2008) and newer libraries constructed from adult coral as well as from different embryonic and larval stages (*A. palmata* NCBI accession numbers GW189124-GW218328; *M. faveolata*, GW246651-GW275983). Expressed sequence tags derived from these cDNA clones were assembled into unique contiguous sequences as previously described (Sunagawa et al. 2009). A representative cDNA clone for each unique sequence was selected for microarray construction; thus, spotted cDNAs represent a random subsample of the transcriptome. See the following references for further details regarding the *A. palmata* sequences (Voolstra et al. 2011) and the new *M. faveolata* microarrays (Aranda et al. 2011). All clone annotations are available via our EST database: http://sequoia.ucmerced.edu/SymBioSys/index.php. Microarray post-processing, hybridization, scanning, and data processing/filtering techniques followed previously published methods (DeSalvo et al. 2010a), and a detailed description can be found in the ESM Text and on Gene Expression Omnibus (GEO series record number GSE27025).

We employed a reference design for each species platform whereby all control and dark-stressed samples (labeled with Cy5) were compared with a pooled reference aRNA sample (labeled with Cy3) composed of aRNA from all fragments. Since all RNA samples were compared with the reference sample, direct comparisons of gene expression across all time points and conditions can be made.

Following data processing and filtering, 9,210 genes of *A. palmata* and 7,184 genes of *M. faveolata* were used for the statistical analyses of gene expression. The ratio between the fluorescence intensity of the two channels was used as input for BAGEL (Bayesian analysis of gene expression levels) (Townsend and Hartl 2002). Genes differentially expressed as a function of darkness stress satisfied the following tests: t0-C = t0-D, t0-C = 9,10d-C, t0-D = 9,10d-C, 9,10d-C ≠ 9,10d-D, t0-D ≠ 9,10d-D, and t0-C ≠ 9,10d-D. In other words, a gene had to be (1) equal among all non-darkness-treated conditions and (2) unequal between the darkness-treated condition (9,10d-D) and all non-darkness-treated conditions. Clustering, principle component analysis, and gene ontology metrics are described in the Supplementary text file (ESM).

Results

Visual observations of bleaching, *Symbiodinium* cell densities and genotyping

Following 1 day of darkness, none of the experimental coral fragments from either species had experienced any noticeable paling in color. After 3 days of darkness, the experimental fragments began to show slight signs of bleaching, and after 4 (*A. palmata*) and 5 (*M. faveolata*) days, experimental fragments had clearly bleached. In order to elicit a further bleaching response, samples were frozen for molecular analyses after 9 (*A. palmata*) and 10 (*M. faveolata*) days of darkness stress.

The visual observations described above point to a faster timeframe for bleaching in *A. palmata* compared with *M. faveolata*. Indeed, this observation is supported by hemocytometer counts to quantify the *Symbiodinium* cell density (Fig. 1). Dark-stressed *A. palmata* have ~75% fewer endosymbionts than both t0 controls ($P < 0.001$) and ~60% fewer endosymbionts than the 9-day controls ($P < 0.05$). Dark-stressed *M. faveolata* have ~50% fewer

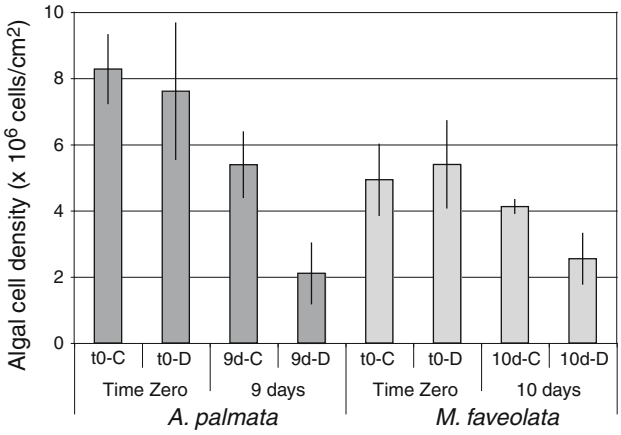

	t0-C	t0-D	9d-C
t0-C			
t0-D	0.8957		
9d-C	**0.0325**	0.1508	
9d-D	**0.0001**	**0.0006**	**0.0152**

	t0-C	t0-D	10d-C
t0-C			
t0-D	0.9452		
10d-C	0.7283	0.4188	
10d-D	**0.0045**	**0.0018**	**0.0279**

Fig. 1 *Symbiodinium* cell counts illustrating bleaching over 9d and 10d in *Acropora palmata* and *Montastraea faveolata*, respectively. Mean cell densities of 4 replicate fragments are shown with SDs. Results of general linear ANOVA models with post hoc pairwise testing via the Tukey HSD method are shown below the *bar graph* for each species

endosymbionts than both t0 controls ($P < 0.005$) and ~40% fewer endosymbionts than the 10-day controls ($P < 0.05$). These results also reveal that the 9- and 10-day control fragments experienced slight bleaching; 9d-C fragments in *A. palmata* have ~30% fewer endosymbionts than both t0 controls ($P < 0.05$ in comparison of 9d-C with t0-C), and 10d-C fragments in *M. faveolata* have ~20% fewer endosymbionts than both t0 controls (though this difference is not statistically significant). Slight bleaching in the 9- and 10-day control fragments is likely due to the low light levels (i.e., shaded ambient light) present during the experiment.

Symbiodinium 18S rRNA gene restriction fragment length polymorphism (RFLP) genotyping analyses revealed that all *A. palmata* fragments house *Symbiodinium* clade A. On the other hand, results in *M. faveolata* were less homogenous. Fragments from colonies 1 and 4 housed clade A, and fragments from colony 2 housed clade C. Colony 3 was highly variable: the t0-C fragment contained clade C; the t0-D fragment contained a mix of clades A and C; and the 10d-C and 10d-D fragments housed clade A.

Transcriptomic responses to darkness stress

In the fragments of *M. faveolata* exposed to darkness stress for 10 days, 21 genes are differentially expressed relative to the control fragments (Fig. 2). Of the 21 genes, 13 genes are down-regulated (fold changes ranging from −1.43 to −2.95) and eight genes are up-regulated (fold changes ranging from +1.18 to +3.42). Nine of the 21 differentially expressed genes (DEGs) are annotated. This transcriptomic response is surprisingly small as only 0.3% of all assayed genes are differentially expressed. On the other hand, in the fragments of *A. palmata* exposed to darkness stress for 9 days, 275 genes are differentially expressed relative to the control fragments (Figs. 3, 4), which represent 3% of all assayed genes. Of the 275 genes, 135 genes are down-regulated (fold changes ranging from −1.27 to −19.73) and 140 genes are up-regulated (fold changes ranging from +1.18 to +9.68). Of the 275 total DEGs, 118 are annotated (43%). Annotations and fold changes for all differentially expressed genes can be found in ESM Tables S1 (*M. faveolata*) and S2 (*A. palmata*).

Because of the 10-fold difference in the number of DEGs between *A. palmata* and *M. faveolata* and the apparent lack of a transcriptomic response to darkness in *M. faveolata*, we performed hierarchical clustering and principal component analysis (PCA) of samples. Both approaches can reveal which factors drive gene expression. As seen in Fig. 5a, *M. faveolata*-stressed samples (i.e., 10d-D) cluster closely with control samples (i.e., t0-C, t0-D, and 10d-C), and four major groups are formed according to host colony. Furthermore, the principal component that explains the most variation partitions the samples by their sampling location—colonies 1 and 2 from Isla Solarte and colonies 3 and 4 from Cayos Zapatillas. These results suggest that the gene expression differences existing between fragments from different colonies and locations were far greater than the differences between control and stressed fragments.

On the other hand, clustering and PCA of *A. palmata* samples (Fig. 5b) reveal why, compared with *M. faveolata*, a greater stress signal is detected. Gene expression in three of the four dark-stressed samples is closely related to each other and distant from all other samples. Moreover, the principal component that explains the most variation

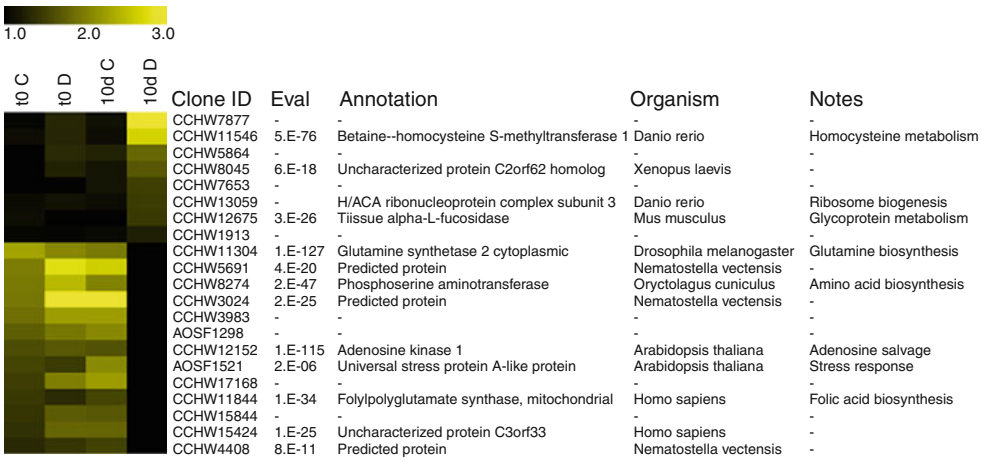

Clone ID	Eval	Annotation	Organism	Notes
CCHW7877	-	-	-	-
CCHW11546	5.E-76	Betaine--homocysteine S-methyltransferase 1	Danio rerio	Homocysteine metabolism
CCHW5864	-	-	-	-
CCHW8045	6.E-18	Uncharacterized protein C2orf62 homolog	Xenopus laevis	-
CCHW7653	-	-	-	-
CCHW13059	-	H/ACA ribonucleoprotein complex subunit 3	Danio rerio	Ribosome biogenesis
CCHW12675	3.E-26	Tiissue alpha-L-fucosidase	Mus musculus	Glycoprotein metabolism
CCHW1913	-	-	-	-
CCHW11304	1.E-127	Glutamine synthetase 2 cytoplasmic	Drosophila melanogaster	Glutamine biosynthesis
CCHW5691	4.E-20	Predicted protein	Nematostella vectensis	-
CCHW8274	2.E-47	Phosphoserine aminotransferase	Oryctolagus cuniculus	Amino acid biosynthesis
CCHW3024	2.E-25	Predicted protein	Nematostella vectensis	-
CCHW3983	-	-	-	-
AOSF1298	-	-	-	-
CCHW12152	1.E-115	Adenosine kinase 1	Arabidopsis thaliana	Adenosine salvage
AOSF1521	2.E-06	Universal stress protein A-like protein	Arabidopsis thaliana	Stress response
CCHW17168	-	-	-	-
CCHW11844	1.E-34	Folylpolyglutamate synthase, mitochondrial	Homo sapiens	Folic acid biosynthesis
CCHW15844	-	-	-	-
CCHW15424	1.E-25	Uncharacterized protein C3orf33	Homo sapiens	-
CCHW4408	8.E-11	Predicted protein	Nematostella vectensis	-

Fig. 2 Heat map of genes that are differentially expressed in *Montastraea faveolata* after 10d of darkness stress. Color scales correspond to BAGEL-computed gene expression estimates where a value of one is assigned to the class with the lowest expression. Clone IDs are searchable in our EST database. Annotations, E-values, and Organism are for the top BLAST hit to the SwissProt database. A *dash* denotes a clone that does not contain BLAST homology to known sequences. The '*Notes*' column reflects protein function as revealed by GO annotation and/or literature searches. In the scale bar: t0, 10d = time; C = control tank; D = dark-treated tank

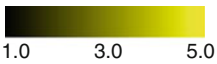

t0 C	t0 D	9d C	9d D	Clone ID	Eval	Annotation	Organism	Notes
				CCHX12763	2.E-17	Protein phosphatase 1 regulatory subunit 3B	Rattus norvegicus	Energy conservation
				CCHX14696	3.E-12	Predicted protein	Nematostella vectensis	-
				CCHX11192	1.E-16	Protein phosphatase 1 regulatory subunit 3B	Rattus norvegicus	Energy conservation
				CAOG655	5.E-93	Betaine--homocysteine S-methyltransferase 1	Xenopus laevis	Homocysteine metabolism
				CCHX1972	6.E-07	Glycine N-methyltransferase (Fragment)	Sus scrofa	Methionine metabolism
				CCHX13810	5.E-100	Inositol oxygenase	Mus musculus	Pentose phosphate pathway
				CCHX16082	5.E-85	10-formyltetrahydrofolate dehydrogenase	Xenopus laevis	Growth arrest
				CCHX12961	4.E-52	Cryptochrome-1	Gallus gallus	Sensory perception
				CCHX12294	3.E-71	Glycine N-methyltransferase	Rattus norvegicus	Methionine metabolism
				CCHX6297	2.E-26	Acid alpha-amylase	Aspergillus niger	-
				CCHX5343	3.E-13	Heat shock protein Hsp-16.2	Caenorhabditis elegans	ER UPR
				CCHX12995	5.E-16	Thyrotroph embryonic factor	Mus musculus	Biological rhythms
				CAOI2197	8.E-39	Hatching enzyme	Paracentrotus lividus	ECM digestion
				CCHX4566	2.E-07	Heat shock protein Hsp-16.1/Hsp-16.11	Caenorhabditis elegans	ER UPR
				CCHX5678	1.E-10	Inositol 2-dehydrogenase	Rhizobium meliloti	Bacterial transcript
				CCHX939	2.E-32	Lipase member K	Homo sapiens	Lipid catabolism
				CCHX12823	7.E-21	Gremlin-1	Rattus norvegicus	Cytokine
				CCHX14203	3.E-22	Cystatin-B	Macaca fuscata fuscata	Cathepsin activity
				CCHX14022	1.E-11	Nose resistant to fluoxetine protein 6	Caenorhabditis elegans	-
				CCHX4531	2.E-08	Chromosome undetermined scaffold_171	Paramecium tetraurelia	-
				AOKF1971	3.E-77	ATP-binding cassette sub-family A member 3	Mus musculus	Lipid transport
				CCHX14701	1.E-71	Actin, cytoskeletal 1A	Strongylocentrotus purpuratus	Actin cytoskeleton
				CAOI2074	1.E-18	cAMP-responsive element-binding protein-like 2	Danio rerio	Transcription factor
				CCHX3687	4.E-08	Heat shock protein Hsp-16.2	Caenorhabditis elegans	ER UPR
				CCHX10197	3.E-47	Lipase member K	Mus musculus	Lipid catabolism
				CAFB1445	2.E-06	Multi EGF-like domains protein 6	Rattus norvegicus	-
				CCHX6047	1.E-11	Universal stress protein A-like protein	Arabidopsis thaliana	Stress response
				CCHX16586	3.E-51	Fibrillin-2	Mus musculus	-
				CCHX12661	4.E-71	Glycine N-methyltransferase	Rattus norvegicus	Methionine metabolism
				CCHX13103	2.E-34	Pecanex-like protein 1	Takifugu rubripes	-
				CAOI1110	2.E-39	Tribbles homolog 2	Homo sapiens	MAPK regulation
				CCHX13489	3.E-13	Cullin-9	Mus musculus	p53 regulation
				CCHX13422	9.E-55	Lipase member K	Mus musculus	Lipid catabolism
				CCHX13059	4.E-06	Death-associated protein kinase 1	Mus musculus	-
				CCHX6144	2.E-73	L-threonine 3-dehydrogenase, mitochondrial	Bos taurus	-
				CCHX15640	2.E-86	Predicted protein	Nematostella vectensis	-
				CCHX13143	4.E-12	Universal stress protein A-like protein	Arabidopsis thaliana	Stress response
				CCHX10336	6.E-24	Predicted protein	Nematostella vectensis	-
				CCHX11438	2.E-29	Protein BTG1	Rattus norvegicus	Growth arrest
				CCHX10071	9.E-38	UDP-glucuronosyltransferase 2B13	Oryctolagus cuniculus	-
				CCHX11094	5.E-06	Putative uncharacterized protein	Branchiostoma floridae	-
				CCHX3916	3.E-23	Sequestosome-1	Pongo abelii	Stress response
				CCHX2338	1.E-57	Dual specificity protein kinase TTK	Mus musculus	Cell division
				AOKF732	1.E-18	Protein BTG2	Homo sapiens	Growth arrest
				CCHX4191	8.E-06	Tenascin-X	Homo sapiens	Cell-ECM adhesion
				CCHX6593	5.E-17	Trace amine-associated receptor 7e	Rattus norvegicus	Orphan receptor
				CCHX8158	5.E-06	Kinesin-like protein unc-104	Drosophila pseudoobscura	Actin cytoskeleton
				CCHX8575	8.E-45	Hypoxia-inducible factor 1-alpha	Gallus gallus	Stress response
				CCHX17033	1.E-35	ATP synth. mito. F1 complex assembly factor 1	Mus musculus	Cell respiration
				CCHX5676	2.E-14	Transmembrane protein 80	Bos taurus	-
				CCHX14486	3.E-13	Protein rolling stone	Drosophila melanogaster	-
				CAOH937	1.E-50	Glutaredoxin-3	Xenopus tropicalis	Stress response
				CCHX16127	1.E-05	E3 ubiquitin-protein ligase MARCH5	Danio rerio	Mitochondrial morphology
				CAOI406	8.E-19	Synaptotagmin-16	Gallus gallus	Vesicle transport
				CCHX6096	8.E-48	Protein ETHE1, mitochondrial	Bos taurus	Cell respiration
				AOKF794	3.E-42	Eukaryotic translation initiation factor 2 subunit 2	Oryctolagus cuniculus	Translation regulation
				CCHX15360	3.E-33	Tetratricopeptide repeat protein 13	Homo sapiens	-
				CAOI1015	2.E-07	MTA/SAH nucleosidase	Exiguobacterium sp.	Bacterial transcript
				CCHX10065	1.E-07	cAMP-responsive element modulator	Bos taurus	Transcription regulation
				CCHX1166	1.E-08	Activating transcription factor 4-like protein	Anthopleura elegantissima	Stress response
				CCHX7120	1.E-16	Predicted protein	Nematostella vectensis	-
				CCHX4786	5.E-17	Usherin	Homo sapiens	Cell-ECM adhesion
				CCHX9020	4.E-31	Probable global transcription activator SNF2L2	Mus musculus	Transcription factor

Fig. 3 Heat map of annotated genes up-regulated 1.5-fold or greater in *Acropora palmata* after 9d of darkness stress. In the *scale bar*: t0, 9d = time; C = control tank; D = dark-treated tank

partitions the samples by sampling time (t0 vs. 9d), which also reveals the coherence of gene expression among three of the four dark-stressed samples. Interestingly, we also see possible variation due to sampling location as the second principle component forms two groups, one consisting of colonies 1 and 2 and another consisting of colonies 3 and 4. Unfortunately, information regarding the reef of origin for *A. palmata* fragments was lost, so we cannot definitively attribute this observation to sampling location.

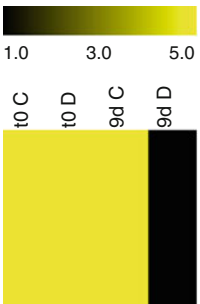

Clone ID	Eval	Annotation	Organism	Notes
CAWS1319	3.E-06	Major yolk protein	Strongylocentrotus purpuratus	Lipid metabolism
CCHX9161	2.E-42	Carbonic anhydrase 2	Oryctolagus cuniculus	Decreased calcification
CAWS688	3.E-09	Serotransferrin	Bos taurus	Iron transport
CCHX1663	7.E-86	GFP-like fluorescent chromoprotein amFP486	Anemonia majano	GFP activity
CCHX15259	5.E-08	Keratin-associated protein 10-12	Homo sapiens	-
CCHX5232	8.E-25	Carbonic anhydrase 2	Oryctolagus cuniculus	Decreased calcification
CCHX13388	1.E-13	Tripartite motif-containing protein 71	Homo sapiens	Developmental protein
CCHX12267	1.E-09	Protein phosphatase 1 regulatory subunit 11	Xenopus laevis	Energy conservation
CAWS1646	2.E-18	Putative uncharacterized protein (Fragment)	Plasmodium chabaudi	Symbiodinium transcript
CCHX13009	1.E-16	Galaxin (Fragment)	Montipora capitata	Decreased calcification
CAWS1657	9.E-24	Predicted protein	Thalassiosira pseudonana	Symbiodinium transcript
CAWS1086	1.E-07	Peridinin-chlorophyll a-binding protein 1, chloroplastic	Amphidinium carterae	Symbiodinium transcript
CCHX9485	2.E-34	Nitrate transporter	Porphyra yezoensis	Symbiodinium transcript
CAWS1514	3.E-16	Peridinin-chlorophyll a-binding protein 1, chloroplastic	Amphidinium carterae	Symbiodinium transcript
CCHX4392	3.E-10	Argininosuccinate lyase 2	Rhizobium loti	Bacterial transcript
CCHX10030	2.E-29	Pantetheinase	Canis familiaris	Pantothenate metabolism
CAWS424	4.E-20	Putative uncharacterized protein	Heterocapsa rotundata	Symbiodinium transcript
CAWS1757	7.E-12	Putative uncharacterized protein (Fragment)	Heterocapsa rotundata	Symbiodinium transcript
CAWS1683	6.E-07	Major basic nuclear protein 2	Crypthecodinium cohnii	Symbiodinium transcript
CAWS1706	2.E-07	Photosystem I reaction center subunit XI	Emiliania huxleyi	Symbiodinium transcript
CCHX2058	8.E-89	Probable saccharopine dehydrogenase	Bos taurus	Amino acid metabolism
CAWS1226	1.E-30	Caroteno-chlorophyll a-c-binding protein (Fragment)	Amphidinium carterae	Symbiodinium transcript
CCHX12280	1.E-10	Predicted protein	Nematostella vectensis	-
CCHX6832	3.E-21	Glutamate [NMDA] receptor-associated protein 1	Bos taurus	-
CCHX11579	1.E-31	Zinc transporter zupT	Oceanobacillus iheyensis	Bacterial transcript
CAWS941	3.E-10	Phosphoenolpyruvate synthase	Deinococcus radiodurans	Bacterial transcript
CAFC1006	1.E-15	Egg protein	Galaxea fascicularis	Lipid metabolism
CAWS789	6.E-12	Putative uncharacterized protein	Clostridium nexile DSM 1787	Symbiodinium transcript
CCHX6222	7.E-08	Putative uncharacterized protein	Perkinsus marinus ATCC 50983	Symbiodinium transcript
CCHX6694	7.E-06	Putative uncharacterized protein (Fragment)	Branchiostoma floridae	-
AOKG735	9.E-23	Putative uncharacterized protein	Desulfobacterium autotrophicum	Bacterial transcript
CCHX9389	2.E-18	E3 ubiquitin-protein ligase TRIM33	Xenopus laevis	Transcription regulation
CAWS1342	2.E-08	Endoplasmin, putative	Perkinsus marinus ATCC 50983	Symbiodinium transcript
CCHX13897	1.E-08	Probable urea active transporter 1	Schizosaccharomyces pombe	Urea transport
CCHX16663	2.E-14	Putative uncharacterized protein	Agrobacterium radiobacter	Bacterial transcript
CCHX10421	2.E-19	Long-chain-fatty-acid--CoA ligase 4	Rattus norvegicus	Lipid metabolism
CCHX16337	8.E-08	Phosphatidylcholine-sterol acyltransferase	Papio anubis	Lipid metabolism
CAWS1381	6.E-22	Fructose-bisphosphate aldolase	Edwardsiella ictaluri (strain 93-146)	Bacterial transcript
CCHX9484	1.E-56	Elongation of very long chain fatty acids protein 4	Mus musculus	Lipid biosynthesis
CAFC2067	4.E-21	Putative uncharacterized protein	Natranaerobius thermophilus	-
CAWS931	1.E-09	Ferredoxin	Peridinium bipes	Symbiodinium transcript
CCHX11553	5.E-44	CAAX prenyl protease 1 homolog	Arabidopsis thaliana	-
CAFC1103	3.E-36	Organic cation transporter protein	Drosophila melanogaster	Cation transport
CCHX9674	8.E-10	Putative tyrosinase-like protein tyr-1	Caenorhabditis elegans	Signal transduction
CAFC1017	1.E-08	Putative uncharacterized protein (Fragment)	Branchiostoma floridae	-
CCHX8739	1.E-27	Heme-binding protein 2	Mus musculus	-
CCHX11168	7.E-06	Putative uncharacterized protein	Perkinsus marinus ATCC 50983	Symbiodinium transcript
CCHX14711	4.E-51	Transmembrane 9 superfamily member 3	Mus musculus	-
CCHX1346	9.E-26	Carbonic anhydrase	Danio rerio	Decreased calcification
CCHX12875	2.E-12	Coiled-coil domain-containing protein 37	Homo sapiens	-
CCHX7519	2.E-67	Actin	Fucus vesiculosus	Actin cytoskeleton
CAOI941	3.E-15	Putative uncharacterized protein	Desulfobacterium autotrophicum	Bacterial transcript
AOKG1439	2.E-09	Nuclear protein 1	Homo sapiens	Growth arrest
CAWS1246	2.E-14	Putative uncharacterized protein	Perkinsus marinus ATCC 50983	Symbiodinium transcript
CCHX7093	1.E-16	Teneurin-3	Mus musculus	Signal transduction
CAFB1950	1.E-27	Putative uncharacterized protein (Fragment)	Branchiostoma floridae	-
CAWS1633	8.E-08	Uncharacterized RNA pseudouridine synthase yhcT	Bacillus subtilis	Bacterial transcript
CCHX13112	4.E-15	2-C-methyl-D-erythritol 4-phosphate cytidylyltransferase	Arabidopsis thaliana	Steriod biosynthesis
CCHX17267	2.E-36	U6 snRNA-associated Sm-like protein LSm7	Mus musculus	Ribosomal protein
CCHX11472	1.E-70	Alkyldihydroxyacetonephosphate synthase, peroxisomal	Cavia porcellus	Lipid biosynthesis
CCHX16444	4.E-18	Predicted protein	Nematostella vectensis	-
CCHX10456	3.E-13	Putative uncharacterized protein	Perkinsus marinus ATCC 50983	-

Fig. 4 Heat map of annotated genes down-regulated 1.5-fold or greater in *Acropora palmata* after 9d of darkness stress. If a transcript is likely of *Symbiodinium* or bacterial origin, then it is noted in the '*Notes*' column

Differentially expressed cellular processes in *A. palmata*

Testing for over-represented gene ontology (GO) terms within lists of DEGs allows for statistical identification of cellular components, molecular functions, and biologic processes implicated in the experimental condition of interest. We used GOEAST (Zheng and Wang 2008) to identify the biologic processes involved in the response to darkness stress in *A. palmata*. GOEAST identified 14 statistically over-represented GO terms among the list of 140 up-regulated DEGs and 12 over-represented GO terms among the 135 down-regulated DEGs (see Table 1 for a condensed list and ESM Table S3 for the complete list of GO terms).

Cellular stress response

Evidence of a potent stress response to darkness includes the over-represented GO terms *transcription factor activity* (GO:0003700) and *ER unfolded protein response* (UPR)

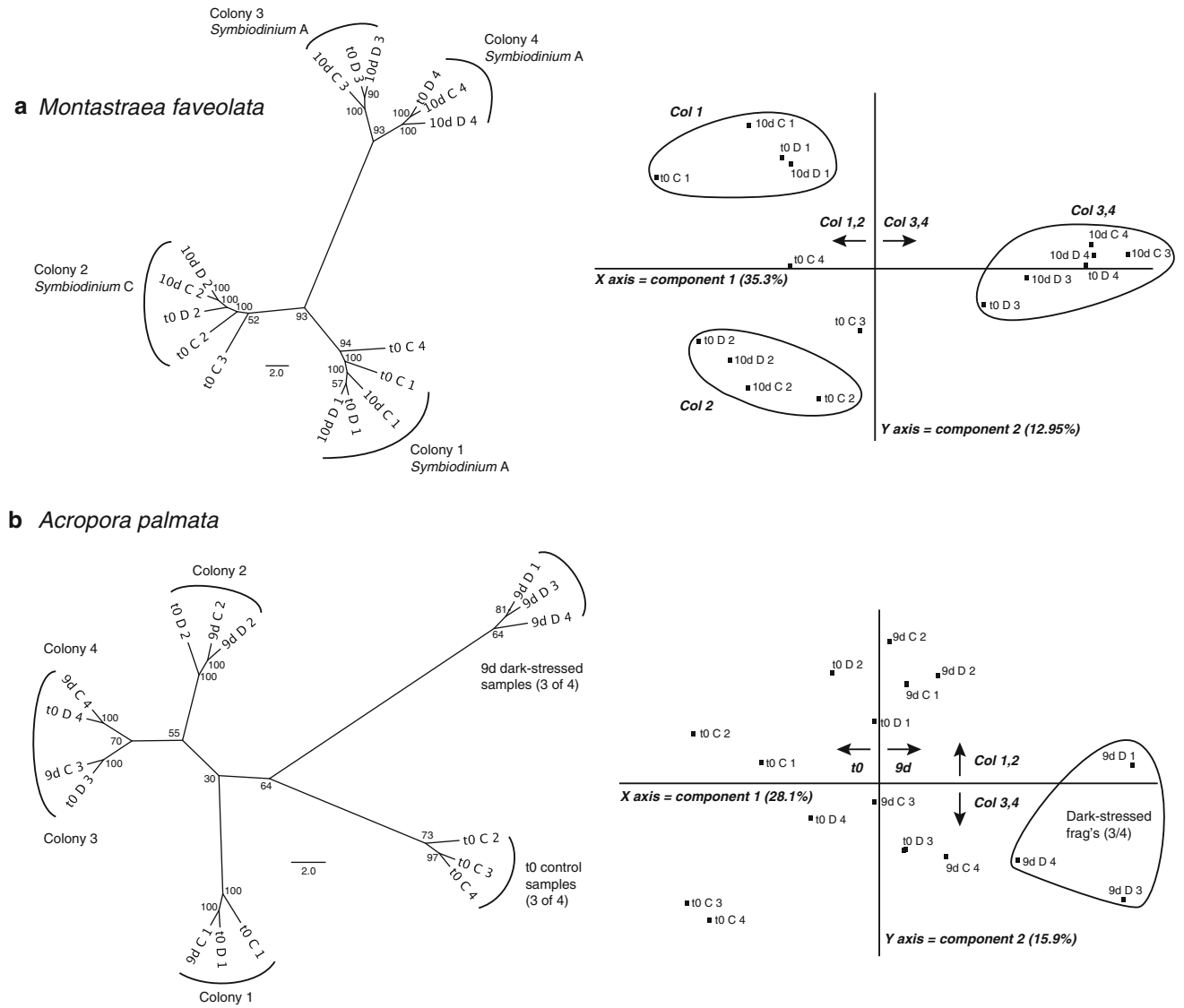

Fig. 5 Hierarchical clustering and principal component analysis (PCA) of gene expression reveal factors that influence gene expression. **a** On the *left*, clustering of *Montastraea faveolata* samples. Dominant *Symbiodinium* clades are included for each colony according to RFLP results. Colonies 1 and 2 were sampled on the same reef (Isla Solarte), as were colonies 3 and 4 (Cayos Zapatillas). On the *right*, PCA of *M. faveolata* samples. **b** On the *left*, clustering of *Acropora palmata* samples. On the *right*, PCA of *A. palmata* samples

(GO:0030968). Stress-responsive transcription factors include (1) cyclic AMP-dependent transcription factor ATF-4 (CCHX1166), which is responsive to oxidative stress and amino acid starvation (Harding et al. 2003), and (2) hypoxia-inducible factor-1α (HIF-1α) (CCHX8575), which is up-regulated when a decrease in cellular oxygen concentration is detected (Semenza 1998). Hypoxic conditions during bleaching are expected given the lack of photosynthetic oxygen generation concomitant with endosymbiont loss. In the *ER UPR* category, three heat shock proteins are up-regulated (CCHX3687, CCHX4566, and CCHX5343). The UPR is a result of ER stress, which occurs from the disruption of normal ER physiology and leads to the accumulation of unfolded proteins within the ER (Li et al. 2006).

Other up-regulated stress-responsive genes not included in the GOEAST results are two universal stress protein A-like proteins (CCHX6047 and CCHX13143); the oxidative stress protein Sequestosome-1 (CCHX3916), which is a molecular biomarker in moon jellies (Schroth et al. 2005); and Glutaredoxin-3 (CAOH937). While the prototypical protein Glutaredoxin-1 senses oxidative stress (Song et al. 2002), the oxidative stress activity of Glutaredoxin-3 is unknown. Lastly, the up-regulation of BTG-1 (CCHX 11438) and BTG-2 (AOKF732) points to growth arrest in dark-stressed *A. palmata* since both of these transcription

Table 1 Selected statistically over-represented gene ontology (GO) categories (as determined using GOEAST) among the differentially expressed genes from the *A. palmata* darkness experiment

GO ID	Ont.	Term	CloneID	E-val	Annotation
Up-regulated					
GO:0003700	MF	Transcription factor activity	AOKF732	1.E-18	Protein BTG2
			CCHX10065	1.E-07	cAMP-responsive element modulator
			CCHX1166	1.E-08	Cyclic AMP-dependent transcription factor ATF-4
			CCHX12995	5.E-16	Thyrotroph embryonic factor
			CCHX8575	8.E-45	Hypoxia-inducible factor 1 alpha
			CCHX9020	4.E-35	Probable global transcription activator SNF2L2
GO:0031965	CC	Nuclear membrane	AOKG2066	7.E-06	Nucleoporin nup189
			CCHX10459	2.E-85	Prickle-like protein 2
GO:0032963	BP	Collagen metabolic process	CAOI2197	8.E-39	Hatching enzyme
			CCHX4191	8.E-06	Tenascin-X
GO:0046983	MF	Protein dimerization activity	CAOI406	8.E-06	Synaptotagmin-16
			CCHX10065	1.E-07	cAMP-responsive element modulator
			CCHX10700	2.E-134	Ras-related GTP-binding protein C
			CCHX1166	1.E-08	Cyclic AMP-dependent transcription factor ATF-4
			CCHX12995	5.E-16	Thyrotroph embryonic factor
			CCHX8575	8.E-45	Hypoxia-inducible factor 1 alpha
GO:0016042	BP	Lipid catabolic process	CCHX10197	3.E-47	Lipase member K
			CCHX13422	9.E-55	Lipase member K
			CCHX939	2.E-32	Lipase member K
GO:0005977	BP	Glycogen metabolic process	CCHX11192	1.E-16	Protein phosphatase 1 regulatory subunit 3B
			CCHX12763	2.E-17	Protein phosphatase 1 regulatory subunit 3B
GO:0030326	BP	Embryonic limb morphogenesis	CCHX12823	7.E-21	Gremlin-1
			CCHX16586	3.E-51	Fibrillin-2
GO:0048511	BP	Rhythmic process	CCHX12961	4.E-52	Cryptochrome-1
			CCHX12995	5.E-16	Thyrotroph embryonic factor
GO:0004033	MF	Aldo–keto reductase activity	CCHX13810	5.E-100	Inositol oxygenase
			CCHX5678	1.E-10	Inositol 2-dehydrogenase
GO:0030968	BP	ER unfolded protein response	CCHX3687	4.E-08	Heat shock protein Hsp-16.2
			CCHX4566	2.E-07	Heat shock protein Hsp-16.1/Hsp-16.11
			CCHX5343	3.E-13	Heat shock protein Hsp-16.2
Down-regulated					
GO:0009507	CC	Chloroplast	CAWS1086	1.E-07	Peridinin-chlorophyll a-binding protein 1, chloroplastic
			CAWS1226	1.E-30	Caroteno-chlorophyll a-c-binding protein (Fragment)
			CAWS1514	3.E-16	Peridinin-chlorophyll a-binding protein 1, chloroplastic
			CAWS1706	2.E-07	Photosystem I reaction center subunit XI
			CAWS931	1.E-09	Ferredoxin
			CCHX13112	4.E-15	2-C-methyl-D-erythritol 4-phosphate cytidylyltransferase, chloroplastic
GO:0018298	BP	Protein–chromophore linkage	CAWS1086	1.E-07	Peridinin-chlorophyll a-binding protein 1, chloroplastic
			CAWS1226	1.E-30	Caroteno-chlorophyll a-c-binding protein (Fragment)
			CAWS1514	3.E-16	Peridinin-chlorophyll a-binding protein 1, chloroplastic
			CCHX1663	7.E-86	GFP-like fluorescent chromoprotein amFP486
GO:0000041	BP	Transition metal ion transport	CAWS1319	3.E-06	Major yolk protein
			CAWS688	3.E-09	Serotransferrin
			CCHX11579	1.E-31	Zinc transporter zupT

Table 1 continued

GO ID	Ont.	Term	CloneID	E-val	Annotation
GO:0031072	MF	Heat shock protein binding	CAWS727	4.E-21	Cysteine string protein
			CCHX15153	5.E-17	DPH4 homolog
GO:0008610	BP	Lipid biosynthetic process	CCHX11472	1.E-70	Alkyldihydroxyacetonephosphate synthase, peroxisomal
			CCHX13112	4.E-15	2-C-methyl-D-erythritol 4-phosphate cytidylyltransferase, chloroplastic
			CCHX9484	1.E-56	Elongation of very long-chain fatty acids protein 4
GO:0004089	MF	Carbonate dehydratase activity	CCHX1346	9.E-26	Carbonic anhydrase
			CCHX5232	8.E-25	Carbonic anhydrase 2
			CCHX9161	2.E-42	Carbonic anhydrase 2

The column 'Ont' refers to the three main ontologies within GO: BP = biologic process; CC = cellular component; and MF = molecular function. Clone IDs are searchable on our EST database. E-values and annotations are for the top BLAST hit to the SwissProt database. A complete list of over-represented GO categories can be found in Table S3

factors are antiproliferative (Winkler 2010). Growth arrest is a hallmark of the cellular stress response (Kultz 2005), and we previously measured up-regulation of AOKF732 in thermal-stressed *A. palmata* (DeSalvo et al. 2010a).

Modification of cellular metabolism

The GOEAST results for up-regulated genes point to dramatic metabolic responses to darkness stress. For example, the GO term *lipid catabolic process* (GO:0016042), represented by Lipase member K (CCHX10197, CCHX13422, and CCHX939), indicates up-regulated lipid hydrolysis. Accordingly, the GO term *lipid biosynthetic process* (GO:0008610) is down-regulated. Given that *Symbiodinium* is responsible for up to 95% of the coral host's fixed carbon pool (Muscatine 1990), it seems reasonable that during bleaching this pool decreases, and thus, the coral host switches to lipids as its main energy source. This idea is supported by numerous studies showing that coral host lipids decrease during stress (e.g., Glynn et al. 1985; Szmant and Gassman 1990; Grottoli et al. 2004; Yamashiro et al. 2005).

In addition, the GO term *glycogen metabolic process* (GO:0005977) is among the up-regulated GO terms represented by two genes with similarity to protein phosphatase 1 (PP1) regulatory subunit 3B, which happen to be the most up-regulated genes in the experiment (+9.68-fold for CCHX12763 and +7.07-fold for CCHX11192). PP1 is a highly conserved eukaryotic gene involved in diverse cellular activities that are regulated by interactions with myriad subunits (Hubbard and Cohen 1993). PP1 regulatory subunit 3B is one such subunit that specifically enhances the rate of PPl-mediated activation of glycogen synthase (Doherty et al. 1995). In pointing to increased glycogen synthesis during bleaching, we must note that this is counterintuitive, since long-term energy storage does not seem likely at a time when the coral's primary energy source (i.e., *Symbiodinium*) is lost and/or dysfunctional. It is possible that (1) in corals, the 3B subunits of PP1 have roles in metabolism that differ from higher eukaryotes or (2) intermediate products in lipid breakdown are being used for gluconeogenesis. Another PP1 subunit, PP1-regulatory subunit 11 (CCHX12267) is ~8-fold down-regulated during darkness stress. PP1-regulatory subunit 11 inhibits PP1 and thus promotes a shift to an energy-conserving state (Ceulemans and Bollen 2004), which is consistent with the idea of the coral host losing its main energy source during bleaching.

Down-regulation of Symbiodinium transcripts

The significantly down-regulated GO terms *chloroplast* (GO:0009507) and *protein–chromophore linkage* (GO:0018298) point to microarray features that derive from *Symbiodinium* mRNA rather than *A. palmata*. This is to be expected given that the cDNA libraries were generated from tissue samples that included symbiotic adults and larvae and that the RNA isolation protocol inevitably leads to some *Symbiodinium* cell lysis. The observed down-regulation of transcripts within both of these categories could arise due to either (1) actual down-regulation of *Symbiodinium* transcripts or (2) the overall loss of *Symbiodinium* cells during the bleaching process. Evidence points to actual down-regulation. We estimated a minimum of 138 microarray features originating from *Symbiodinium* based on their top BLAST hits being dinoflagellate sequences. Fifty-five of these genes passed our filtering criteria, and 18 were differentially expressed, all down-regulated. If this signal was due to less *Symbiodinium* RNA input in bleached samples, then we would expect all 55 genes to be down-regulated. Furthermore, actual down-regulation of chlorophyll-binding proteins is expected given that darkness causes a decrease in total proteins, nucleic acids, and chlorophyll in plants (Choudhury and Biswal 1979).

The only non-*Symbiodinium* transcript within the GO term *protein–chromophore linkage* is the GFP-like fluorescent chromoprotein amFP486 (CCHX1663). This finding is

consistent with previous studies showing GFP down-regulation during stress (DeSalvo et al. 2008; Smith-Keune and Dove 2008).

Decreased calcification

Also consistent with previous findings is the down-regulated GO term *carbonate dehydratase activity* (GO:0004089) represented by three carbonic anhydrase transcripts (CCHX1346, CCHX5232, and CCHX9161). The diminished activity of carbonic anhydrase, which catalyzes the hydration of CO_2 to HCO_3^-, indicates decreased calcification during stress since this enzyme is thought to regulate calcium carbonate deposition in scleractinian corals (e.g., Goreau 1959; Tambutte et al. 2007) and/or act as a CO_2 supply mechanism during the assimilation of photosynthetic carbon (Weis et al. 1989). Furthermore, the down-regulation of Galaxin transcripts (CCHX13009) also points to decreased calcification during darkness stress. Galaxin localizes to the organic matrix of *Galaxea fascicularis* (Fukuda et al. 2003), and Galaxin transcripts in *Acropora millepora* exhibit in situ hybridization staining patterns consistent with calcification (Reyes-Bermudez et al. 2009). Decreased calcification during thermal stress was previously suggested by transcriptomic responses in *A. palmata* and *M. faveolata* (DeSalvo et al. 2008, 2010a) and was shown directly in response to thermal stress (e.g., Jokiel and Coles 1977) and darkness stress (Goreau 1959; Al-Horani et al. 2007).

Overlap between A. palmata and M. faveolata

Despite very little differential gene expression in dark-stressed *M. faveolata*, there is, interestingly, one gene consistently up-regulated in both *M. faveolata* and *A. palmata*: Betaine-homocysteine S-methyltransferase 1 (BHMT) (CAOG655 in *A. palmata* and CCHW11546 in *M. faveolata*). BHMT simultaneously converts betaine to dimethylglycine and homocysteine to methionine. Up-regulation of BHMT suggests increased production of methionine, perhaps due to decreased transfer of this amino acid from endosymbiont to host. An alternative explanation is that the up-regulation of BHMT is indicative of increased betaine concentrations in the host cell during stress since betaine, as an osmolyte, protects cells, proteins, and enzymes from environmental stress (Craig 2004). This brings up the possibility of BHMT functioning in osmoregulation, and indeed, in rat hepatic cells, BHMT was up-regulated during hypo-osmotic stress and down-regulated during hyperosmotic stress (Schafer et al. 2007). Osmotic stress has received attention in the context of coral bleaching as an example of hyperosmotic stress (Mayfield and Gates 2007), and thus, we would expect to see BHMT down-regulated. Nonetheless, the activity of BHMT and the broader metabolism of betaine, homocysteine, and the amino acids synthesized as a result of this pathway ought to be researched in the future. After all, given the evidence that free amino acids appear to act as a 'host factor' for photosynthate release (Gates et al. 1995) and that tight shuttling of metabolites between host and symbiont is vital to the maintenance of the symbiosis (Trench 1979), bleaching mechanisms are likely to be intricately woven with metabolic pathways.

Comparison between thermal and darkness bleaching in A. palmata

Since darkness stress elicited a marked response in *A. palmata*, a comparison with its thermal stress response (DeSalvo et al. 2010a) represents an opportunity to understand core cellular stress responses in corals. Interestingly, only nine DEGs overlap between the two studies. This paucity of overlap likely reflects technical differences such as (1) the thermal bleaching study was completed with small microarrays ($\sim$2,000 features), whereas the current study utilized microarrays with >10,000 features and (2) sources of technical variance such as quality of hybridization and data filtering methods lead to different experiments being represented by different lists of genes from which DEGs are identified. Nevertheless, viewing the DEGs from the broader perspective of cellular processes reveals prominent parallels between the darkness and thermal stress responses in *A. palmata*. For example, both stressors elicit the following cellular responses: (1) chaperone up-regulation; (2) antioxidant up-regulation; (3) growth arrest; and (4) decreased calcification. The first three responses are expected given their involvement in the conserved cellular stress response, and down-regulation of putative calcification genes reflects published observations of decreased calcification following thermal or darkness stress. Perhaps more interesting are the nine DEGs overlapping between the two studies. Strikingly, the direction and magnitude of change for these genes are nearly identical between the two studies. Down-regulated genes include two non-annotated genes (AOKF1228 and AOFG735). Up-regulated genes include three non-annotated genes (AOKF2019, AOKG2067, and CAOI854) and four annotated genes. The annotated up-regulated genes include eukaryotic translation initiation factor 2 subunit 2 (AOKF794), ATP-binding cassette subfamily A member 3 (AOKF1971, a lipid transporter), Protein BTG2 (AOKF732, a negative regulator of the cell cycle), and Synaptotagmin-16 (CAOI406, involved in membrane trafficking and signal transduction). That these genes are differentially expressed consistently during heat- and dark-induced bleaching argues for future studies into their mechanism of action.

Discussion

Gene expression microarrays represent powerful tools to elucidate molecular responses that underlie physiologic conditions of interest. In this study, we used cDNA microarrays to investigate the transcriptomic responses to darkness stress in *M. faveolata* and *A. palmata*. Although further biochemical and protein-level analyses will be necessary in order to follow up on the activities of the DEGs described herein, the present investigations yielded a number of interesting results.

While darkness elicited a visual bleaching response in both species, a transcriptomic stress signature was observed in *A. palmata* (275 DEGs) but not in *M. faveolata* (21 DEGs). This striking difference between species is discussed below, but we begin by discussing the cellular effects of darkness on *Symbiodinium* and coral host.

The cellular effects of darkness stress on host and symbiont

Numerous abiotic stresses (e.g., UV radiation, dark, heat, cold, and salinity) trigger coral bleaching. For example, severe cold stress in the coral *Montipora digitata* causes a decrease in photosynthetic efficiency, changes in photosynthetic pigment concentrations, photodamage, bleaching, and increased mortality (Saxby et al. 2003). All of these symptoms also occur during thermal stress; thus, it seems reasonable to posit that multiple triggers may elicit common molecular mechanisms leading to bleaching. Regarding the most studied stressor (thermal stress alone or in synergy with solar radiation), the etiology of bleaching is thought to begin in the endosymbiont with photoinhibition of electron transport in the thylakoid membranes, which subsequently damages photosystem II and leads to ROS production (Smith et al. 2005). Thus, a valid question is as follows: "Do other triggers elicit the same chain of events in the chloroplast?"

This question is difficult to answer since most coral stress studies are concerned with thermal stress, and not all studies measure photosynthetic efficiency and ROS formation/antioxidant responses. However, we can look to plant physiologic studies, and there is evidence that both darkness and cold stress cause photodamage in plants. During darkness stress in maize seedlings, steady decomposition of stroma lamellae is followed by unstacking and destruction of thylakoids, which leads to declines in photoelectron transport efficiency and CO_2 fixation (Choudhury and Biswal 1979). Furthermore, during cold stress in soybean shoots, unstacking of chloroplast grana occurs, as does a decrease in photosynthetic efficiency (Musser et al. 1984). In addition, cold stress in maize seedlings leads to ROS formation and oxidative stress (Prasad et al. 1994).

Given that darkness stress in plants causes photodamage and that darkness-induced gene expression in *A. palmata* shows a potent stress response involving chaperone activity, growth arrest, and antioxidant up-regulation (also seen during thermal stress), we propose that the underlying trigger leading to dark-induced bleaching is similar to (if not the same as) that described above for thermal stress. Taking into account the results of Saxby et al. (2003), we also expect cold stress to share common gene expression signatures with thermal and darkness stress. These notions set up testable hypotheses to address (1) whether dark stress causes photoinhibition and ROS formation in zooxanthellate corals and (2) whether cold stress–induced transcriptomic responses are similar to those in the present study. With regard to the latter point, we note that using microarray technology to study bleaching triggers other than cold stress (such as UV radiation and salinity) is equally important.

The above discussion centered on the probable cellular effects of darkness stress on *Symbiodinium*. On the other hand, how does darkness stress affect the coral host? Oxygen concentrations in coral tissues are remarkably elevated due to algal photosynthesis (Dykens and Shick 1982). These concentrations follow diel patterns concomitant with solar radiation and algal photosynthesis (Levy et al. 2006), which means that coral tissue becomes hypoxic in the dark (Shashar et al. 1993; Kühl et al. 1995). Thus, experimental darkness treatment inevitably causes hypoxia in the coral host. Indeed, our results reflect this—HIF-1α is nearly twofold up-regulated in dark-treated *A. palmata*.

Hypoxia and the ER unfolded protein response are critical cellular events involved in the bleaching response

Comparing the results of the present study with our earlier studies on thermal stress in *A. palmata* and *M. faveolata* (DeSalvo et al. 2008, 2010a), it is clear that both darkness and thermal stress elicit the following cellular responses: (1) chaperone up-regulation; (2) antioxidant up-regulation; (3) growth arrest; (4) metabolic modifications; and (5) decreased calcification. In positing how both thermal stress and darkness stress might converge on the aforementioned cellular responses, we must determine how darkness-induced photosynthesis dysfunction in *Symbiodinium* and subsequent hypoxia in the coral host are related to the canonical view of ROS production by *Symbiodinium* and subsequence oxidative stress–induced death of both host and symbiont cells.

Previous studies have highlighted the importance of Ca^{2+} homeostasis as a cellular process that can lead to the myriad downstream responses observed during thermal

stress and bleaching (Sandeman 2006; DeSalvo et al. 2008). Furthermore, many genes differentially expressed during ultraviolet radiation stress in coral larvae were related to Ca^{2+} homeostasis (Aranda et al. 2011). Interestingly, the up-regulated GO category *ER unfolded protein response* (UPR) is a cellular process that has not received attention in the context of coral bleaching, and below, we illustrate how hypoxia, the ER UPR, and Ca^{2+} homeostasis are intricately linked via oxidative stress and the activity of ATF-4 (which is up-regulated in thermal- and dark-stressed *A. palmata*).

Consider the following notions: (1) the prevailing mechanism of coral bleaching involves the cytotoxic effects of oxidative stress (reviewed in Lesser 2006); (2) oxidative stress in general disrupts ER function; (3) both ER stress and oxidative stress lead to an increase in cytosolic Ca^{2+}; and (4) increased cytosolic Ca^{2+} increases ROS generation in the mitochondria (reviewed in Malhotra and Kaufman 2007). Here is the connection to hypoxia: HIF-1 is hydroxylated and thereby inactive during normoxia due to the action of oxygen-sensing prolyl-4-hydroxylase domain enzymes, but during hypoxia, mitochondrial ROS inhibit HIF-1 hydroxylation leading to HIF-1 activation (Maltepe and Saugstad 2009).

ATF-4 fits into this picture because it is up-regulated following ER stress, amino acid starvation, and hypoxia. This signaling pathway begins with the stress-induced activation of kinases that phosphorylate eukaryotic initiation factor 2 (eIF2α), which negatively regulates the translation of most mRNAs but selectively up-regulates the translation of ATF-4 (Harding et al. 2000). One such kinase that activates eIF2α is PKR-like endoplasmic reticulum kinase (PERK), an ER stress protein that is also activated during prolonged hypoxia (Ye and Koumenis 2009). Interestingly, a clone spotted on the *A. palmata* microarray with homology to PERK (CCHX5386) is up-regulated 2.8-fold and 1.9-fold in dark-treated *A. palmata* relative to t0C and t0D controls, respectively. Once up-regulated, ATF-4 alleviates amino acid starvation and ER stress by activating the transcription of chaperones, antioxidant proteins, and amino acid metabolism proteins (reviewed in Rutkowski and Kaufman 2003). Consequently, cells lacking ATF-4 are more susceptible to ER stress, amino acid deficiency, and oxidative stress, leading to increased cell death (Harding et al. 2003).

Thus, the putative sequential mechanism of bleaching is the following: ROS production by *Symbiodinium*, oxidative and ER stress in the coral host, an increase in cytosolic Ca^{2+}, mitochondrial ROS formation, hypoxia and further oxidative stress, and cell death. An outstanding question related to the present study is whether darkness causes ROS production in *Symbiodinium*. If so, then oxidative stress and hypoxia might converge to cause a breakdown of Ca^{2+} homeostasis, ER stress, and ATF-4 up-regulation. On the other hand, it is possible that hypoxia is the primary stress response in darkness-treated corals leading to the myriad differentially expressed genes documented here. Lastly, while hypoxia is especially relevant during darkness-induced bleaching given the prolonged absence of photosynthesis, we must note that as corals progressively bleach from other stressors, hypoxic conditions will likely develop as more and more symbiont cells are lost from host tissue.

Why is there no darkness stress signature in *M. faveolata*?

The results from hierarchical clustering and PCA of gene expression data (Fig. 5) indicate why only 21 genes are differentially expressed in *M. faveolata* compared with 275 genes differentially expressed in *A. palmata*. In the case of *M. faveolata* (Fig. 5a), stress-induced gene expression is over-ridden by gene expression differences due to collection site, host colony, and possibly *Symbiodinium* clade. Despite two outliers, fragments of *M. faveolata* cluster by host colony, and the principal component that explains the most variation (35%) groups samples by their sampling location. Interestingly, the distance between colony 1 (harboring *Symbiodinium* clade A) and colony 2 (harboring *Symbiodinium* clade C) in the HCL tree is greater than the distance between colonies 3 and 4 (both harboring *Symbiodinium* clade A), and this is supported by the grouping of samples according to the second principle component. These last observations point to a slight symbiont influence on the gene expression data, which is consistent with our previous study on *M. faveolata* (DeSalvo et al. 2010b). However, why is gene expression in this study shaped more by sampling location than symbiont genotype? We attribute this discrepancy to the differing geographic scales of the two studies. In our previous study, we sampled five different host colonies from the same reef, all within swimming distance of each other. In that case, environmental histories/conditions were consistent. In the present study, we sampled colonies at two different sites 21 km apart; thus, environmental histories/conditions were dissimilar. It thus appears that measuring gene expression in corals sampled from a wide geographic area can cloud an investigator's ability to measure differential gene expression. Indeed, similar results were found when measuring heat stress–induced differential gene expression in *M. faveolata* larvae sampled in Florida and Mexico (Polato et al. 2010).

Overall, our results point to the power of comparative studies. For example, by studying both *A. palmata* and *M. faveolata*, it is clear that coral species with differing life histories respond to disturbance differently and have varying degrees of stress sensitivity. Thus, we must be cautious in making claims on how corals will respond to climate change

based on the physiologic measurements of a single coral species. Investigating the diversity of responses within and between species is crucial to accurately forecast the affects of future environmental insults on corals.

Acknowledgments We thank the following people associated with STRI in Panamá: R. Collin, G. Jácome, P. Gondola, and other staff at the Bocas del Toro station and E. Gomez and J. Jara at the Naos Laboratory. We also thank M. A. Coffroth for initial input with tank experiments and the many members of the Medina Lab responsible for cDNA microarray construction. Lastly, we thank three anonymous reviewers whose comments greatly improved the manuscript. This study was supported through an STRI Pre-doctoral Fellowship and an NSF award to M.D. (OISE 0837455) and NSF awards to M.M. (BE-GEN 0313708 and IOS 0644438). This is contribution #4 of the STRI Caribbean Reef Futures initiative.

References

Al-Horani FA, Tambutte E, Allemand D (2007) Dark calcification and the daily rhythm of calcification in the scleractinian coral, *Galaxea fascicularis*. Coral Reefs 26:531–538

Aranda M, Banaszak AT, Bayer T, Luyten JR, Medina M, Voolstra CR (2011) Differential sensitivity of coral larvae to natural levels of ultraviolet radiation during the onset of larval competence. Mol Ecol 20:2955–2972

Brown BE (1997) Coral bleaching: causes and consequences. Coral Reefs 16:S129–S138

Ceulemans H, Bollen M (2004) Functional diversity of protein phosphatase-1, a cellular economizer and reset button. Physiol Rev 84:1–39

Choudhury NK, Biswal UC (1979) Changes in photoelectron transport of chloroplasts isolated from dark stressed leaves of maize seedlings. Experientia 35:1036–1037

Craig SA (2004) Betaine in human nutrition. Am J Clin Nutr 80:539–549

DeSalvo MK, Voolstra CR, Sunagawa S, Schwarz JA, Stillman JH, Coffroth MA, Szmant AM, Medina M (2008) Differential gene expression during thermal stress and bleaching in the Caribbean coral *Montastraea faveolata*. Mol Ecol 17:3952–3971

DeSalvo MK, Sunagawa S, Voolstra CR, Medina M (2010a) Transcriptomic responses to heat stress and bleaching in the elkhorn coral *Acropora palmata*. Mar Ecol Prog Ser 402:97–113

DeSalvo MK, Sunagawa S, Fisher PL, Voolstra CR, Iglesias-Prieto R, Medina M (2010b) Coral host transcriptomic states are correlated with *Symbiodinium* genotypes. Mol Ecol 19:1174–1186

Doherty MJ, Moorhead G, Morrice N, Cohen P, Cohen PTW (1995) Amino-acid-sequence and expression of the hepatic glycogen-binding (G(L))-subunit of protein phosphatase-1. FEBS Lett 375:294–298

Douglas AE (2003) Coral bleaching–how and why? Mar Pollut Bull 46:385–392

Downs CA, Kramarsky-Winter E, Martinez J, Kushmaro A, Woodley CM, Loya Y, Ostrander GK (2009) Symbiophagy as a cellular mechanism for coral bleaching. Autophagy 5:211–216

Dunn SR, Bythell JC, Le Tissier MDA, Burnett WJ, Thomason JC (2002) Programmed cell death and cell necrosis activity during hyperthermic stress-induced bleaching of the symbiotic sea anemone *Aiptasia* sp. J Exp Mar Biol Ecol 272:29–53

Dunn SR, Thomason JC, Le Tissier MD, Bythell JC (2004) Heat stress induces different forms of cell death in sea anemones and their endosymbiotic algae depending on temperature and duration. Cell Death Differ 11:1213–1222

Dunn SR, Schnitzler CE, Weis VM (2007) Apoptosis and autophagy as mechanisms of dinoflagellate symbiont release during cnidarian bleaching: every which way you lose. Proc R Soc Lond, Ser B: Biol Sci 274:3079–3085

Dykens JA, Shick JM (1982) Oxygen production by endosymbiotic algae controls superoxide-dismutase activity in their animal host. Nature 297:579–580

Fukuda I, Ooki S, Fujita T, Murayama E, Nagasawa H, Isa Y, Watanabe T (2003) Molecular cloning of a cDNA encoding a soluble protein in the coral exoskeleton. Biochem Biophys Res Commun 304:11–17

Gates RD, Baghdasarian G, Muscatine L (1992) Temperature stress causes host cell detachment in symbiotic cnidarians: implications for coral bleaching. Biol Bull 182:324–332

Gates RD, Hoegh-Guldberg O, McFall-Ngai MJ, Bil KY, Muscatine L (1995) Free amino acids exhibit anthozoan "host factor" activity: they induce the release of photosynthate from symbiotic dinoflagellates in vitro. Proc Natl Acad Sci USA 92:7430–7434

Glynn PW, Perez M, Gilchrist SL (1985) Lipid decline in stressed corals and their crustacean symbionts. Biol Bull 168:276–284

Goreau TF (1959) The physiology of skeleton formation in corals. I. A method for measuring the rate of calcium deposition by corals under different conditions. Biol Bull 116:59–75

Grottoli AG, Rodrigues LJ, Juarez C (2004) Lipids and stable carbon isotopes in two species of Hawaiian corals, *Porites compressa* and *Montipora verrucosa*, following a bleaching event. Mar Biol 145:621–631

Grottoli AG, Rodrigues LJ, Palardy JE (2006) Heterotrophic plasticity and resilience in bleached corals. Nature 440:1186–1189

Harding HP, Novoa I, Zhang Y, Zeng H, Wek R, Schapira M, Ron D (2000) Regulated translation initiation controls stress-induced gene expression in mammalian cells. Mol Cell 6:1099–1108

Harding HP, Zhang Y, Zeng H, Novoa I, Lu PD, Calfon M, Sadri N, Yun C, Popko B, Paules R, Stojdl DF, Bell JC, Hettmann T, Leiden JM, Ron D (2003) An integrated stress response regulates amino acid metabolism and resistance to oxidative stress. Mol Cell 11:619–633

Higuchi T, Fujimura H, Hitomi Y, Arakaki T, Oomori T, Suzuki Y (2011) Photochemical formation of hydroxyl radicals in tissue extracts of the coral *Galaxea fascicularis*. Photochem Photobiol 86:1421–1426

Hoegh-Guldberg O (1999) Climate change, coral bleaching and the future of the world's coral reefs. Mar Freshw Res 50:839–866

Hubbard MJ, Cohen P (1993) On target with a new mechanism for the regulation of protein-phosphorylation. Trends Biochem Sci 18:172–177

Jokiel PL, Coles SL (1977) Effects of temperature on the mortality and growth of Hawaiian reef corals. Mar Biol 1977:201–208

Kühl M, Cohen Y, Dalsgaard T, Jorgensen BB, Revsbech NP (1995) Microenvironment and photosynthesis of zooxanthellae in scleractinian corals studied with microsensors for O_2, pH and light. Mar Ecol Prog Ser 117:159–172

Kultz D (2005) Molecular and evolutionary basis of the cellular stress response. Annu Rev Physiol 67:225–257

Lesser MP (1996) Elevated temperatures and ultraviolet radiation cause oxidative stress and inhibit photosynthesis in symbiotic dinoflagellates. Limnol Oceanogr 41:271–283

Lesser MP (2006) Oxidative stress in marine environments: biochemistry and physiological ecology. Annu Rev Physiol 68: 253–278

Levy O, Achituv Y, Yacobi YZ, Dubinsky Z, Stambler N (2006) Diel 'tuning' of coral metabolism: physiological responses to light cues. J Exp Biol 209:273–283

Li J, Lee B, Lee AS (2006) Endoplasmic reticulum stress-induced apoptosis: multiple pathways and activation of p53-up-regulated modulator of apoptosis (PUMA) and NOXA by p53. J Biol Chem 281:7260–7270

Malhotra JD, Kaufman RJ (2007) The endoplasmic reticulum and the unfolded protein response. Semin Cell Dev Biol 18:716–731

Maltepe E, Saugstad OD (2009) Oxygen in health and disease: regulation of oxygen homeostasis–clinical implications. Pediatr Res 65:261–268

Mayfield AB, Gates RD (2007) Osmoregulation in anthozoan-dinoflagellate symbiosis. Comp Biochem Physiol, A: Mol Integr Physiol 147:1–10

Muscatine L (1990) The role of symbiotic algae in carbon and energy flux in reef corals. In: Dubinsky Z (ed) Ecosystems of the world 25: Coral reefs. Elsevier, Amsterdam, pp 75–87

Musser RL, Thomas SA, Wise RR, Peeler TC, Naylor AW (1984) Chloroplast ultrastructure, chlorophyll fluorescence, and pigment composition in chilling-stressed soybeans. Plant Physiol 74: 749–754

Nii CM, Muscatine L (1997) Oxidative stress in the symbiotic sea anemone *Aiptasia pulchella* (Carlgren, 1943): Contribution of the animal to superoxide ion production at elevated temperature. Biol Bull 192:444–456

Polato NR, Voolstra CR, Schnetzer J, DeSalvo MK, Randall CJ, Szmant AM, Medina M, Baums IB (2010) Location-specific responses to thermal stress in larvae of the reef-building coral *Montastraea faveolata*. PLoS One 5:e11221

Prasad TK, Anderson MD, Martin BA, Stewart CR (1994) Evidence for chilling-induced oxidative stress in maize seedlings and a regulatory role for hydrogen-peroxide. Plant Cell 6:65–74

Reyes-Bermudez A, Lin ZY, Hayward DC, Miller DJ, Ball EE (2009) Differential expression of three galaxin-related genes during settlement and metamorphosis in the scleractinian coral *Acropora millepora*. BMC Evol Biol 9:178

Rowan R, Knowlton N (1995) Intraspecific diversity and ecological zonation in coral-algal symbiosis. Proc Natl Acad Sci USA 92:2850–2853

Rowan R, Powers DA (1991) Molecular genetic identification of symbiotic dinoflagellates (zooxanthellae). Mar Ecol Prog Ser 71:65–73

Rutkowski DT, Kaufman RJ (2003) All roads lead to ATF4. Dev Cell 4:442–444

Sandeman IM (2006) Fragmentation of the gastrodermis and detachment of zooxanthellae in symbiotic cnidarians: a role for hydrogen peroxide and Ca2 + in coral bleaching and algal density control. Rev Biol Trop 54:79–96

Saragosti E, Tchernov D, Katsir A, Shaked Y (2011) Extracellular production and degradation of superoxide in the coral *Stylophora pistillata* and cultured *Symbiodinium*. PLoS One 5:e12508

Saxby T, Dennison WC, Hoegh-Guldberg O (2003) Photosynthetic responses of the coral *Montipora digitata* to cold temperature stress. Mar Ecol Prog Ser 248:85–97

Schafer C, Hoffmann L, Heldt K, Lornejad-Schafer MR, Brauers G, Gehrmann T, Garrow TA, Haussinger D, Mayatepek E, Schwahn BC, Schliess F (2007) Osmotic regulation of betaine homocysteine-S-methyltransferase expression in H4IIE rat hepatoma cells. Am J Physiol Gastrointest Liver Physiol 292:G1089–G1098

Schroth W, Ender A, Schierwater B (2005) Molecular biomarkers and adaptation to environmental stress in moon jelly (*Aurelia* spp.). Mar Biotechnol 7:449–461

Schwarz JA, Brokstein PB, Voolstra C, Terry AY, Miller DJ, Szmant AM, Coffroth MA, Medina M (2008) Coral life history and symbiosis: functional genomic resources for two reef building caribbean corals, *Acropora palmata* and *Montastraea faveolata*. BMC Genomics 9:97

Semenza GL (1998) Hypoxia-inducible factor 1: master regulator of O_2 homeostasis. Curr Opin Genet Dev 8:588–594

Shashar N, Cohen Y, Loya Y (1993) Extreme diel fluctuations of oxygen in diffusive boundary-layers surrounding stony corals. Biol Bull 185:455–461

Smith DJ, Suggett DJ, Baker NR (2005) Is photoinhibition of zooxanthellae photosynthesis the primary cause of thermal bleaching in corals? Global Change Biol 11:1–11

Smith-Keune C, Dove S (2008) Gene expression of a green fluorescent protein homolog as a host-specific biomarker of heat stress within a reef-building coral. Mar Biotechnol 10:166–180

Song JJ, Rhee JG, Suntharalingam M, Walsh SA, Spitz DR, Lee YJ (2002) Role of glutaredoxin in metabolic oxidative stress. Glutaredoxin as a sensor of oxidative stress mediated by H_2O_2. J Biol Chem 277:46566–46575

Steen RG, Muscatine L (1987) Low-temperature evokes rapid exocytosis of symbiotic algae by a sea-anemone. Biol Bull 172:246–263

Strychar KB, Coates M, Sammarco PW, Piva TJ (2004) Bleaching as a pathogenic response in scleractinian corals, evidenced by high concentrations of apoptotic and necrotic zooxanthellae. J Exp Mar Biol Ecol 304:99–121

Sunagawa S, Wilson EC, Thaler M, Smith ML, Caruso C, Pringle JR, Weis VM, Medina M, Schwarz JA (2009) Generation and analysis of transcriptomic resources for a model system on the rise: the sea anemone *Aiptasia pallida* and its dinoflagellate endosymbiont. BMC Genomics 10:258

Szmant AM, Gassman NJ (1990) The effects of prolonged "bleaching" on the tissue biomass and reproduction of the reef coral *Montastrea annularis*. Coral Reefs 8:217–224

Tambutte S, Tambutte E, Zoccola D, Caminiti N, Lotto S, Moya A, Allemand D, Adkins J (2007) Characterization and role of carbonic anhydrase in the calcification process of the azooxanthellate coral *Tubastrea aurea*. Mar Biol 151:71–83

Tchernov D, Gorbunov MY, de Vargas C, Yadav SN, Milligan AJ, Haggblom M, Falkowski PG (2004) Membrane lipids of symbiotic algae are diagnostic of sensitivity to thermal bleaching in corals. Proc Natl Acad Sci USA 101:13531–13535

Tchernov D, Kvitt H, Haramaty L, Bibby TS, Gorbunov MY, Rosenfeld H, Falkowski PG (2011) Apoptosis and the selective survival of host animals following thermal bleaching in zooxanthellate corals. Proc Natl Acad Sci USA 108:9905–9909

Townsend JP, Hartl DL (2002) Bayesian analysis of gene expression levels: statistical quantification of relative mRNA level across multiple strains or treatments. Genome Biol 3:RESEARCH0071

Trench RK (1979) The cell biology of plant-animal symbiosis. Annu Rev Plant Physiol 30:453–485

Voolstra CR, Sunagawa S, Matz MV, Bayer T, Aranda M, Buschiazzo E, Desalvo MK, Lindquist E, Szmant AM, Coffroth MA, Medina M (2011) Rapid evolution of coral proteins responsible for interaction with the environment. PLoS One 6:e20392

Wang J-T, Meng P-J, Sampayo EM, Tang S-L, Chen CA (2011) Photosystem II breakdown induced by reactive oxygen species in freshly-isolated *Symbiodinium* from *Montipora* (Scleractinia; Acroporidae). Mar Ecol Prog Ser 422:51–62

Weis VM (2008) Cellular mechanisms of Cnidarian bleaching: stress causes the collapse of symbiosis. J Exp Biol 211:3059–3066

Weis VM, Smith GJ, Muscatine L (1989) A "CO_2 supply" mechanism in zooxanthellate cnidarians: role of carbonic-anhydrase. Mar Biol 100:195–202

Winkler GS (2010) The mammalian anti-proliferative BTG/Tob protein family. J Cell Physiol 222:66–72

Yamashiro H, Oku H, Onaga K (2005) Effect of bleaching on lipid content and composition of Okinawan corals. Fish Sci 71:448–453

Ye J, Koumenis C (2009) ATF4, an ER stress and hypoxia-inducible transcription factor and its potential role in hypoxia tolerance and tumorigenesis. Curr Mol Med 9:411–416

Zheng Q, Wang XJ (2008) GOEAST: a web-based software toolkit for Gene Ontology enrichment analysis. Nucleic Acids Res 36:W358–W363